Check for updates

ChemElectroChem

Research Article
doi.org/10.1002/celc.202300557

Chemistry Europe
European Chemical Societies Publishing

www.chemelectrochem.org

Electrochemical and Photoelectrochemical Bimodal Sensor Based on Copper Modified g-C_3N_4 for Nitrate Detection

Wafa Aidli,*[a] Daniele Fumagalli,[a] Hanieh Helli,[a] Luigi Falciola,*[a] and Valentina Pifferi[a]

Nitrates (NO_3^-) are crucial in agricultural practices and the food industry, but their excessive presence in water can lead to adverse health effects. Their leaching into water sources necessitates regular monitoring. This study introduces a novel bimodal electrochemical (EC)/photoelectrochemical (PEC) sensor, utilizing copper-modified graphitic carbon nitride (Cu/g-C_3N_4), designed for precise nitrate determination. The structural morphology and chemical composition of the Cu/g-C_3N_4 nanocomposite were meticulously examined using Transmission Electron Microscopy (TEM) and Fourier-transform infrared spectroscopy (FTIR). The optimization of copper loading in g-C_3N_4 was conducted, and the electrochemical behavior and light irradiation interaction of various Cu/g-C_3N_4 nanocomposites were systematically studied. The investigation revealed that 20% Cu/g-C_3N_4 represented the optimal doping ratio, establishing the most promising candidate for NO_3^-. Nitrates were consistently measured using both EC and PEC techniques, yielding Limits of Detection (LoD) of 3.75 and 9.60 ppm, respectively. The sensor's robust performance was further demonstrated in the presence of possible interferents. The proposed sensors were also successfully used to detect NO_3^- in commercial water. This bimodal sensor presents a promising approach for accurate nitrate determination, attesting to its potential for effective cross-validation.

Introduction

Nitrates represent an ubiquitous source of nitrogen naturally present in ecosystems and an essential part of the nitrogen cycle.[1] They are also used as key components of synthetic fertilizers for plant growth and food production for humans and animals.[2] In normal circumstances, nitrates exhibit beneficial effects on human health, promoting increased blood flow, reducing blood pressure, and preventing cardiovascular diseases.[3] However, due to their intensive and extensive use not only as fertilizers,[4] their quantity has significantly increased in water and soil, causing detrimental impacts on both the environment and human health. From an environmental perspective, nitrates contribute to the phenomenon of eutrophication and play a role in the increase of nitric oxide, one of the gases responsible for the greenhouse effect.[5] From a health perspective, a high intake of nitrates from water and food can result in adverse effects on the endocrine system, potentially leading to the onset of diseases such as Parkinson's and Alzheimer's,[6,7] Moreover, in the vulnerable digestive systems of children, it can manifest as specific syndromes, including the infamous "blue-baby" syndrome.[8] To mitigate these problems, the World Health Organization (WHO) recommends a maximum contaminant level of 50 ppm NO_3^- (50 mg L^{-1}) in drinking water to safeguard public health.[9]

Driven by these concerns, researchers have directed their efforts towards two pivotal areas: the removal of nitrates from water and their precise analytical quantification.

The removal of nitrates has been a hot research topic, with various techniques explored, such as adsorption, reverse osmosis, advanced filtration, and biological denitrification.[10] However, these methods often come with high operating costs or the potential to generate secondary pollutants. Recently, attention has pivoted towards photocatalytic reduction as a sustainable removal method. Numerous studies have investigated semiconducting catalysts for NO_3^- photocatalytic reduction, encompassing metal oxides (e.g., TiO_2[11]), sulfides (e.g., CdS,[12] ZnS[13]), and perovskites (e.g., $GdCrO_3$,[14] $BaLa_4Ti_4O_{15}$[15]). Graphitic carbon nitride (g-C_3N_4), a metal-free semiconductor, has lately regained popularity owing to its exceptional efficiency, cost-effectiveness, chemical stability, and ease of modification. Successful nitrate photocatalytic reduction using g-C_3N_4 has been demonstrated, marking a promising advancement in sustainable removal methodologies.[16]

Regarding nitrate detection, traditional quantification methods such as spectrophotometric,[17] chromatographic,[18] electrophoretic,[19] colorimetric[20] and fluorescence[21] techniques have long been employed. Despite their effectiveness, these methods present challenges, including high costs, prolonged analysis times, complexity, and the need for sample pretreatments, making them less suitable for on-site applications.

In the pursuit of developing assays that offer rapid, cost-effective, and user-friendly solutions, electrochemical techniques have emerged as promising tools for nitrate sensing. Given the electroactive nature of nitrates,[22] various electro-

[a] W. Aidli, D. Fumagalli, H. Helli, L. Falciola, V. Pifferi
Electroanalytical Chemistry Group, Department of Chemistry
Università degli Studi di Milano
Via Golgi 19, 20133, Milano, Italy
E-mail: wafa.aidli@unimi.it
luigi.falciola@unimi.it
Homepage: sites.unimi.it/ELAN

Supporting information for this article is available on the WWW under https://doi.org/10.1002/celc.202300557

© 2024 The Authors. ChemElectroChem published by Wiley-VCH GmbH. This is an open access article under the terms of the Creative Commons Attribution License, which permits use, distribution and reproduction in any medium, provided the original work is properly cited.

© 2024 The Authors. ChemElectroChem published by Wiley-VCH GmbH

chemical methods have been devised, relying on the electroreduction process.[23,24] Researchers have explored a spectrum of nanomaterials, with a particular emphasis on noble metals (e.g., Au, Pd, Ag)[25–27] and transitional metals (e.g., Zn, Cu)[28,29] in crafting sensitive and selective nitrate electrochemical sensors.

Copper, in particular, stands out due to its exceptional catalytic activity in nitrate reduction, coupled with high conductivity, all while maintaining cost-effectiveness and affordability. Furthermore, the versatility of copper extends to its capacity for easy integration with various other materials, allowing for the creation of different structures that contribute to enhanced performance.[30–32]

However, despite the undeniable advantages of electrochemical methods in terms of ease and speed of use, they, like all other techniques, are susceptible to interferents and matrix effects present in real samples, leading to a reduction in accuracy during practical applications.[33]

To face these challenges, a growing trend in sensors design towards the integration of different transduction modes into one sensor. These sensors, often referred to as 'bimodal' or 'dual-mode' sensors, leverage the versatile properties of nanomaterials to combine various sensing techniques such as electrochemical-colorimetric,[34] electrochemical-electrochemiluminescent,[35] electrochemical-photoelectrochemical,[36] fluorescent-electrochemical,[37] fluorescent-colorimetric[38] methodologies.

The adoption of this dual-mode approach, was found to provide a cross-validation of analytical results, thereby enhancing the reliability of the sensor.[39]

In this context, we introduced a novel bimodal electrochemical-photoelectrochemical (EC-PEC) sensor for the detection of nitrates based on copper modified graphitic carbon nitride (Cu/g-C_3N_4). The choice of the nanomaterial is driven by the dual electrocatalytic and photocatalytic properties of copper and graphitic carbon nitride, respectively, towards nitrate reduction. The primary analytical focus of this sensor is the determination of NO_3^- at neutral pH through electrochemical reduction. Operating in PEC mode involves conducting measurements under UV LED irradiation, ensuring optimal photoactivation. The EC and PEC outputs mutually reinforce each other, providing more reliable results than single-mode sensing. While nitrate electrochemical sensing has been extensively studied, to the best of our knowledge, this work marks the first reported instance of photoelectrochemical nitrate sensing.

Results and Discussion

Materials Characterization

The synthesis process of the copper-modified graphitic carbon nitride (Cu-g-C_3N_4) active material and its subsequent immobilization on a conductive Fluorine-doped Tin Oxide (FTO) electrode are elucidated in Figure 1. Comprehensive material characterization was conducted at each stage of the electrode preparation.

Characterization of both pristine and Cu-modified g-C_3N_4 was performed using FTIR, as reported in Figure 2A. The presence of C–N heterocycles is confirmed by the trigonal C–N(–C)–C and bridging C–NH–C stretching signals between 952 cm^{-1} and 1601 cm^{-1}. The sharp peak at 792 cm^{-1} confirms the presence of the typical g-C_3N_4 structure, attributed to the breathing mode of the tri-s-triazine units,[40] Additionally, the broad absorption band at 3074 cm^{-1} validates the composition of g-C_3N_4, representing the stretching vibration of N–H/H–N–H.[41]

Upon modification with copper, all characteristic vibrational peaks related to pristine g-C_3N_4 are retained, suggesting that the structural integrity of graphitic carbon nitride remained intact. Although the three IR spectra appear very similar, small differences can be seen upon careful examination. This includes the appearance of a new weak absorption band at 2176 cm^{-1} attributed to the formation of C≡N triple bonds, a common defect site originating from the opening of triazine rings. This suggests that copper is chemically coordinated to the g-C_3N_4 host, most likely in the form of Cu–N bonds within the in-plane cavities of g-C_3N_4. These observations are typical in metal doped g- and align with findings reported in previous studies on metal doped g-C_3N_4.[42,43]

As a comparative analysis we examined the as-prepared pure copper and observed a characteristic peak at 597 cm^{-1}, corresponding to the Cu–O bonds in the Cu_2O structure.[44] The absence of this peak in the Cu/g-C_3N_4 spectrum confirms the presence of Cu in its most stable, single-atom form.

Exfoliated g-C_3N_4 was studied with TEM imaging (Figure 2C), confirming the presence of 2D porous layered nanosheets. The structure was amorphous, and the single sheet size was in the range of hundreds of nanometers. TEM analysis of the Cu-g-C_3N_4 material reveals similar graphitic stacking structures, indicating that the fundamental morphology remains largely unaffected after copper doping. The nanosheets appeared more densely packed, featuring increased pore density and smaller sheet sizes. Such a behavior is common when single atom metal is introduced into the structure.[45,46] The absence of clusters further supports the proposition that atomic copper is incorporated into the g-C_3N_4 structure, rather than the formation of discrete copper or copper oxide particles.[47]

The electrochemical characterization was conducted following the immobilization of the prepared materials on Fluorine-doped Tin Oxide (FTO) glass slides. Initially, cyclic voltammetry was performed in Na_2SO_4. Figure 3A and 3B illustrate the results, where Cyclic Voltammetry reveals no peaks for bare g-C_3N_4. In contrast, distinct Cu oxidation and reduction peaks are observable in the copper-doped g-C_3N_4, providing clear confirmation of successful copper incorporation.

Next Electrochemical Impedance Spectroscopy (Figure 3D, the fitted parameters obtained with the inset circuit are reported in Table S1) in the presence of 5 mM $[Fe(CN)_6]^{3-/4-}$ as redox probe.

Nyquist spectra showed that the charge transfer resistance of g-C_3N_4, which corresponds to the diameter of the semicircle, decreased when the Cu percentage was raised from 5% to 30%

© 2024 The Authors. ChemElectroChem published by Wiley-VCH GmbH

21960216, 0, Downloaded from https://chemistry-europe.onlinelibrary.wiley.com/doi/10.1002/celc.202300557 by Universita'Degli Studi Di Mila, Wiley Online Library on [27/11/2024]. See the Terms and Conditions (https://onlinelibrary.wiley.com/terms-and-conditions) on Wiley Online Library for rules of use; OA articles are governed by the applicable Creative Commons License

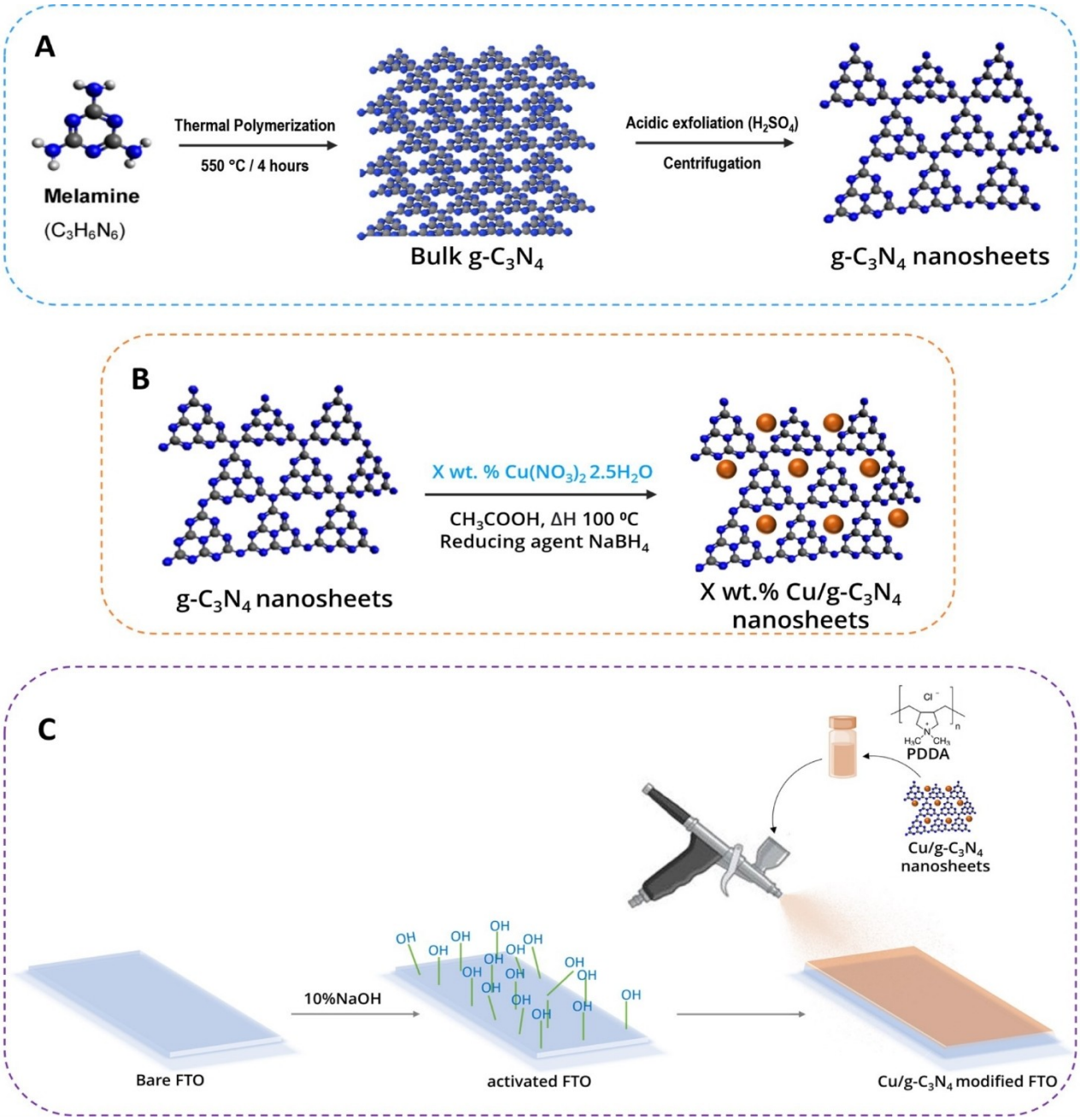

Figure 1. Schematic representation of the (A) synthesis of g-C_3N_4 nanosheets, (B) its modification with copper and (C) the immobilization on a conductive glass slide to be used as electrode.

in comparison to pristine g-C_3N_4. This indicates that Cu doping increases the conductivity of g-C_3N_4 significantly.

Increasing the percentage to 40% led to excessive loading, leading to higher resistance again. This effect is attributed to the shielding of the surface's active sites, suggesting that there exists an optimal Cu percentage for maximizing conductivity without causing excessive loading.

Interestingly, the resistance of both 20%wt and 30%wt Cu/g-C_3N_4 was lower than that of pure Cu_2O. This finding implies that g-C_3N_4 provides a high specific surface area with abundant accessible Cu–N active sites in comparison to bulk copper, highlighting the synergistic effect between copper and graphitic carbon nitride.

These results were further confirmed by cyclic voltammetry recorded in the presence of the ferrocyanide probe (Figure 3C). The high peak-to-peak separation of 0.45 V in bare g-C_3N_4 was successfully reduced to 0.14 V, and the current intensity followed the same pattern observed for the charge transfer resistance, with the best value obtained at 20%wt Cu/g-C_3N_4, while a decrease was observed at higher concentrations.

Photoactivity of the nanomaterials was evaluated using irradiation with a 395 nm LED. As shown in Figure 4A, Bare g-

© 2024 The Authors. ChemElectroChem published by Wiley-VCH GmbH

21960216, 0, Downloaded from https://chemistry-europe.onlinelibrary.wiley.com/doi/10.1002/celc.202300557 by Universita'Degli Studi Di Mila, Wiley Online Library on [27/11/2024]. See the Terms and Conditions (https://onlinelibrary.wiley.com/terms-and-conditions) on Wiley Online Library for rules of use; OA articles are governed by the applicable Creative Commons License

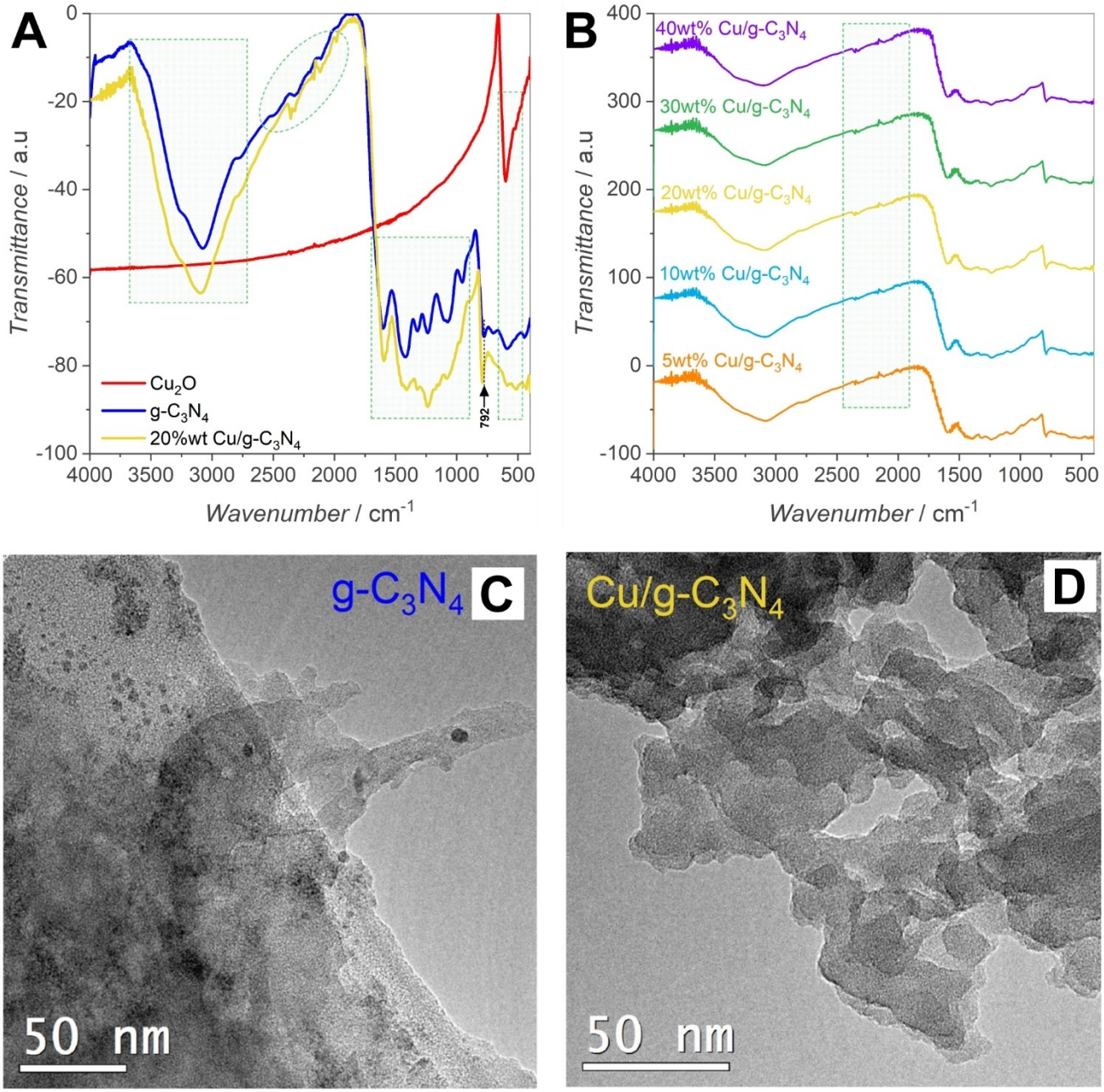

Figure 2. FTIR specta of Cu_2O, g-C_3N_4 and the 20% Cu/g-C_3N_4 (A) and of the composite material with different percentages of copper (B). TEM images of exfoliated g-C_3N_4 (C) and Cu/g-C_3N_4 (D).

C_3N_4 showed a low photocurrent of only 1.023 μA, due to low efficiency of the electron-hole separation. Cu_2O, thanks to its lower band gap and better electron transfer kinetic, reached 2 μA of intensity. The best results were achieved with the copper modified g-C_3N_4, in particular with 20%wt Cu/g-C_3N_4 whose intensity was 39 times higher than that of pure g-C_3N_4. This can be explained with the formation of a p-n heterojunction which improves carriers' separation and electron transfer kinetics. Notably, the signal remained stable for multiple cycles, indicating the stability of the nanomaterial. Given the results obtained from both photoactivity and electrochemical measurements, the 20 wt% Cu/g-C_3N_4 sample was selected for further analytical detection experiments.

Nitrate Studies

Nitrate reduction with the prepared electrodes was initially evaluated using CV. Figure 4B the characteristic cathodic peak at −0.8 V, corresponding to the reduction reaction:

$$NO_3^- + 2H^+ + 2e^- \rightarrow NO_2^- + H_2O$$

© 2024 The Authors. ChemElectroChem published by Wiley-VCH GmbH

21960216, 0, Downloaded from https://chemistry-europe.onlinelibrary.wiley.com/doi/10.1002/celc.202300557 by Universita'Degli Studi Di Mila, Wiley Online Library on [27/11/2024]. See the Terms and Conditions (https://onlinelibrary.wiley.com/terms-and-conditions) on Wiley Online Library for rules of use; OA articles are governed by the applicable Creative Commons License

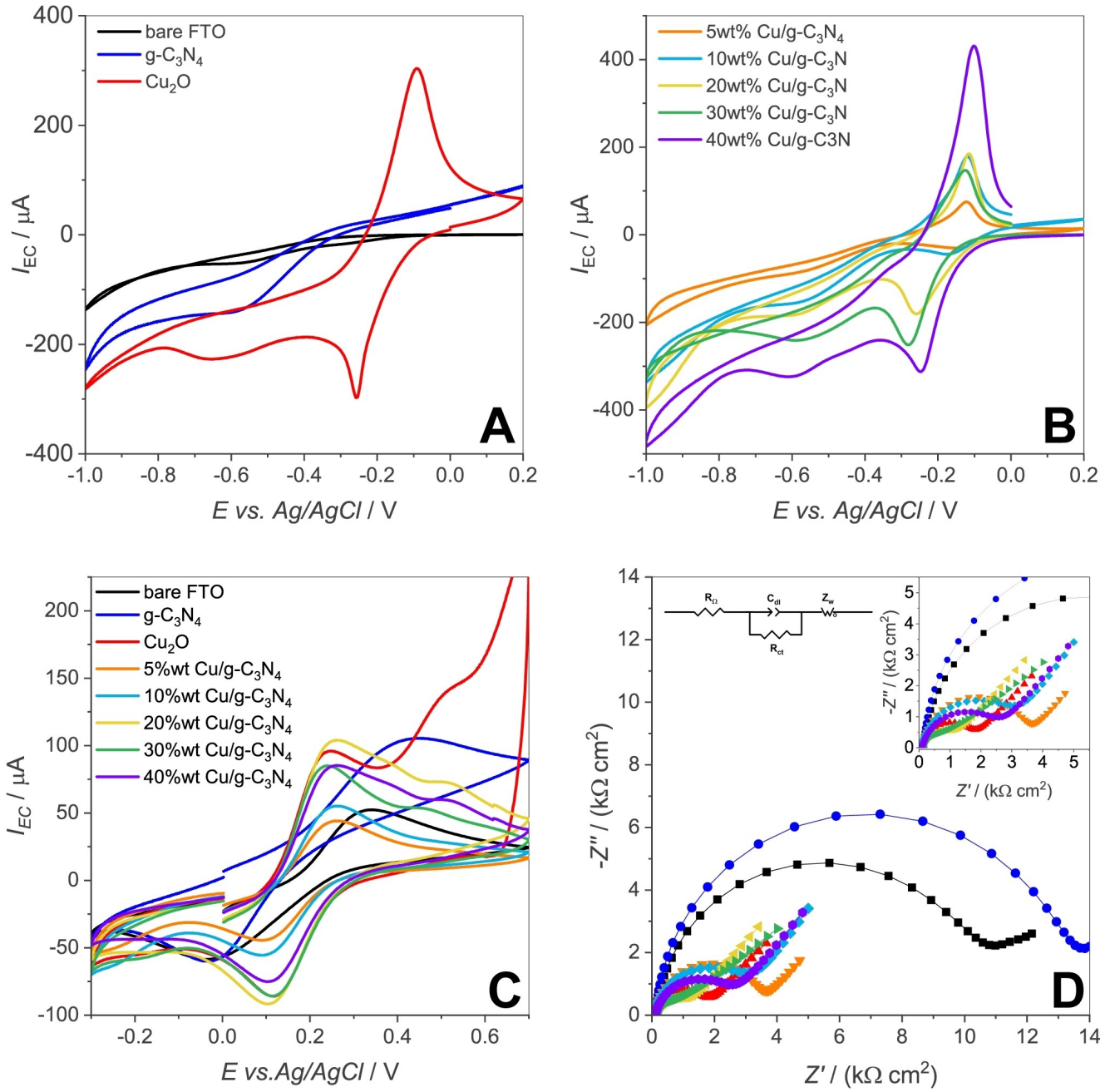

Figure 3. Cyclic voltammograms of FTO electrodes modified with (A) pure g-C_3N_4 and Cu_2O and (B) different nanocomposites in 0.1 M Na_2SO_4 (pH 6.0). (C) Cyclic voltammograms and (D) Nyquist plot curves of modified electrodes recorded in a 0.1 M KCl containing 5 mM $[Fe(CN)_6]^{3-/4-}$.

The peak intensity was found to be significantly influenced by the copper loading ratio, with the 20%wt Cu/g-C_3N_4 composite exhibiting the highest current response.

This trend was consistently observed in photoelectrochemical (PEC) analysis, where various modified electrodes exhibited a cathodic photocurrent signal. Notably, a substantial enhancement was observed in the presence of nitrate ions, with the 20% doping ratio demonstrating the highest intensity (Figure 4C).

Nitrate detection was performed using the 20%wt Cu/g-C_3N_4 modified FTO electrode. The bimodal nature of the sensor allowed us to establish a calibration line using both electrochemical methods, Linear Sweep Voltammetry (LSV), and PEC. In Figure 5A, the LSV results exhibit a clear increase in the reduction peak at −0.78 V, revealing two linear ranges for concentrations between 10–100 ppm and 100–200 ppm. The Limit of Detection (LoD) was calculated as 3.75 ppm (S/N = 3.29) (Figure 5A, inset). For PEC analysis, a single linear range was observed between 10 and 200 ppm, and the corresponding Limit of Detection was calculated as 9.60 ppm (S/N = 3.29) (Figure 5B and inset). The obtained values are compared with other literature works in Table 1. Notably, the preparation of the

© 2024 The Authors. ChemElectroChem published by Wiley-VCH GmbH

21960216, 0, Downloaded from https://chemistry-europe.onlinelibrary.wiley.com/doi/10.1002/celc.202300557 by Universita'Degli Studi Di Mila, Wiley Online Library on [27/11/2024]. See the Terms and Conditions (https://onlinelibrary.wiley.com/terms-and-conditions) on Wiley Online Library for rules of use; OA articles are governed by the applicable Creative Commons License

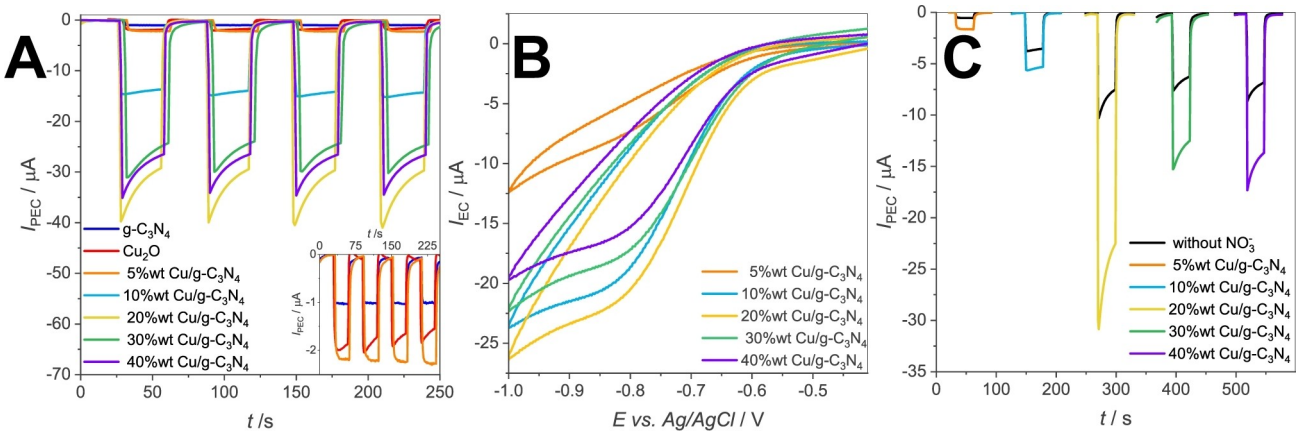

Figure 4. (A) Photocurrent responses of different nanocomposites at 0 V in 0.1 M Na_2SO_4 under intermittent 395 nm LED irradiation. (B) EC (cyclic voltammetry, 50 mV s^{-1}) and (C) PEC (chronoamperometry, 0 V vs Ag/AgCl) measurements recorded in Na_2SO_4 in the presence of 100 µM $NaNO_3$.

Table 1. Summary of the performances of other nitrate sensors present in the literature.

Method	Sensing matrix	pH/Cell purging	Linear Range (ppm)	LOD (ppm)	Reference
LSV	Copper nanowire	2.0/N_2 purging	1.24–155	1.48	[50]
CV	Ag NPs/Au electrode	5.0/N_2 purging 5.0/N_2 purging	0.62–620	1.48 0.62	[27]
LSV	Cu nanowires	2.0/N_2 purging	0.5–363	0.08	[48]
CA	Pd NPs/epoxy–Cu	7.0/No purging	2–35	N.A	[51]
LSV	Pd–Cu/SWCN SPE	2.0/No purging	6.2–124	3.23	[52]
CA	CNTs/PPYs/NiR	7.5/N_2 purging	27–90	10	[53]
DPV	Pd NCs–PPy	7.0/No purging	6.2–49 55–86	0.05 0.03	[26]
LSV	Inkjet-printed Ag	8.0/No purging	1–200	1.40	[54]
LSV-PEC	Cu/g-C_3N_4	6.0/No purging	10–200	3.75 and 9.60	This work

sensor presented in this work is easier than that of most of other works, the cost of the components is lower, and the working conditions are at neutral pH, while the sensors based on copper are usually optimized for very acidic pH. Furthermore, according to our knowledge, no prior reports were found about PEC sensing of nitrates. As shown in Figure 5C–D and S1, the presence of interferents such as NO_2^-, SO_4^{2-}, Ca^{2+}, Cu^{2+}, Cl^-, Na^+, Mg^{2+} and HCO_3^- was negligible, as expected for copper-modified sensors.[48,49] Along interference effects, the stability of the device was evaluated (Figure S2) as a key parameter for environmental monitoring applications. Overall, this sensor proved to be robust and reliable. The sensor's response was tested with real samples, analyzing commercial bottled water.

As reported in Table 2, EC and PEC measurements were very consistent, reporting values which deviated less than 3.10% from the labeled ones. The matrix effects of the real samples did not affect the performances of the sensor, with apparent recovery factors ranging from 98.16% to 101.69% and from 98.03% to 100.77% for EC and PEC measurements, respectively.

Conclusions

In this work, a bimodal electrochemical-photoelectrochemical sensor based on copper-modified g-C_3N_4 was designed specifically for the determination of nitrates in an aqueous environment and was extensively compared with pristine g-C_3N_4 and Cu_2O. Both electrochemical and photoelectrochemical characterizations demonstrated superior performance with the Cu doped g-C_3N_4, particularly at a 20% copper loading. The 20%wt Cu/g-C_3N_4 exhibited the best analytical performance for nitrate determination, achieving Limit of Detection (LoD) values of 3.75 and 9.60 ppm with EC and PEC methods, respectively, without interference from major matrix species. Real water sample analyses demonstrated excellent apparent recovery factors and an efficient cross-validation method, highlighting the efficacy of the bimodal sensor.

© 2024 The Authors. ChemElectroChem published by Wiley-VCH GmbH

21960216, 0, Downloaded from https://chemistry-europe.onlinelibrary.wiley.com/doi/10.1002/celc.202300557 by Universita'Degli Studi Di Mila, Wiley Online Library on [27/11/2024]. See the Terms and Conditions (https://onlinelibrary.wiley.com/terms-and-conditions) on Wiley Online Library for rules of use; OA articles are governed by the applicable Creative Commons License

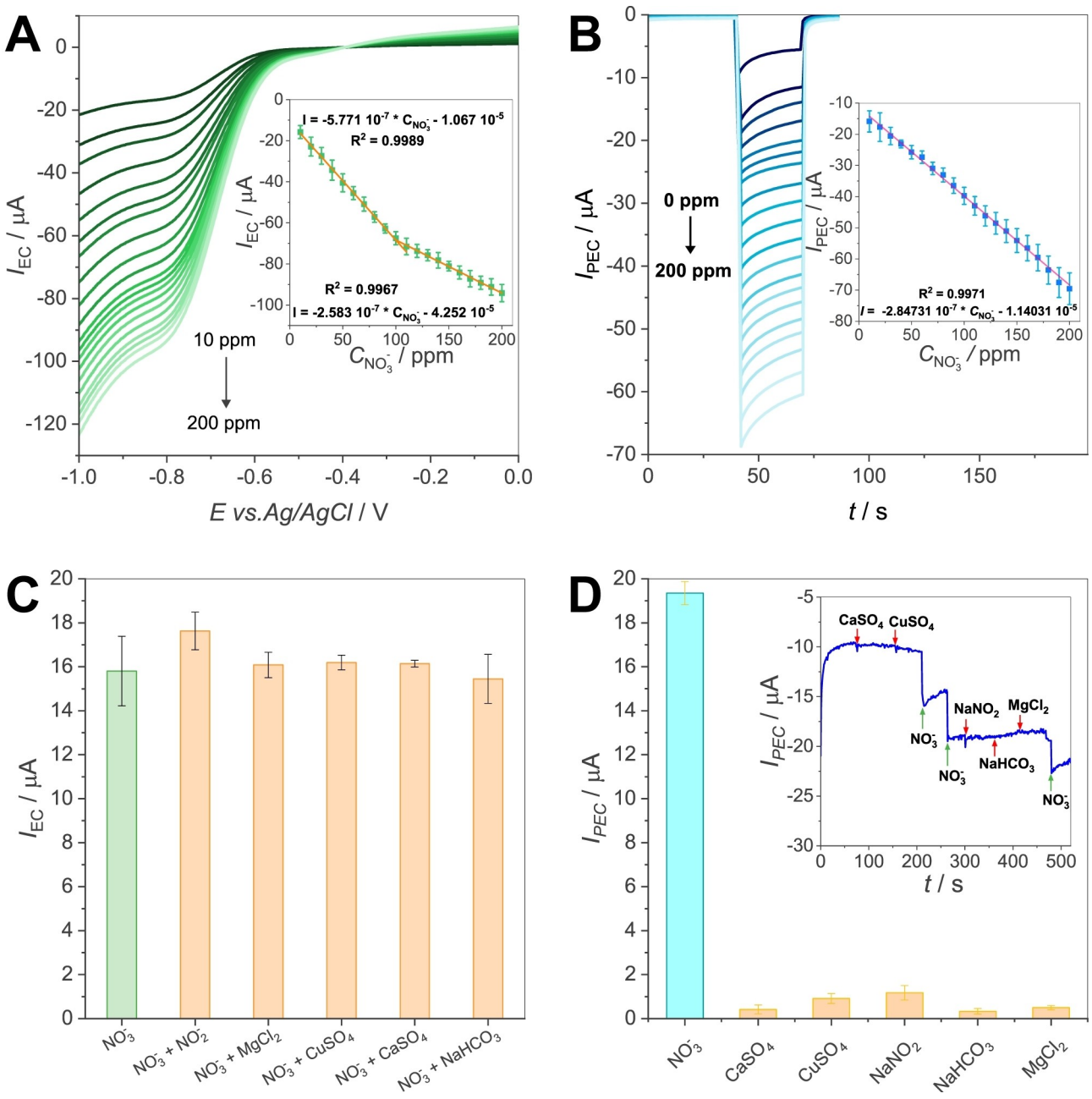

Figure 5. EC (Linear Sweep Voltammetry, 20 mV s^{-1}) and PEC (Chronoamperometry, 0 V vs Ag/AgCl) recorded with consecutive additions of $NaNO_3$. The corresponding calibration lines are reported as inset. (C) EC and (D) PEC response in presence of interferents, chronoamperometry response reported as inset.

Experimental Section

Reagents

Melamine (99%), Sulfuric Acid (98%), Copper(II) nitrate hemi(pentahydrate) (98%), Acetic Acid (glacial, ≥99.7%), Sodium hydroxide (97%), Poly(diallyldimethylammonium chloride) solution (20wt. % in H2O), Sodium hydroxide (≥97.0%), Ethanol (≥99.8%), Acetone (≥99.5%), Sodium Sulfate (≥99.0%), Sodium Nitrate ((≥99.0%), Potassium hexacyanoferrate(II) trihydrate (98.5–102.0%) and Potassium chloride (99.0–100.5%) were purchased from Sigma-Aldrich and used without further purification. Water for the preparation of the solutions was doubly distilled (conductivity: 0.055 µS cm^{-1}) purified by a MilliQ apparatus.

Synthesis of g-C_3N_4 Nanosheets

To synthesize bulk g-C_3N_4, thermal condensation of melamine was used.[55] Briefly, 6 g of melamine were heated at 550 °C for 4 hours with a temperature ramp of 3 °C min^{-1}. The obtained yellow powder (1 g) was later exfoliated:[42] after one night of stirring in 30 mL of H_2SO_4, the solution was poured in 100 mL of water and sonicated for 2 hours. The obtained white powder was separated by centrifugation (9000 rpm, 10 min) rinsed with water to neutral pH and dried at 60° overnight.

© 2024 The Authors. ChemElectroChem published by Wiley-VCH GmbH

21960216, 0, Downloaded from https://chemistry-europe.onlinelibrary.wiley.com/doi/10.1002/celc.202300557 by Universita'Degli Studi Di Mila, Wiley Online Library on [27/11/2024]. See the Terms and Conditions (https://onlinelibrary.wiley.com/terms-and-conditions) on Wiley Online Library for rules of use; OA articles are governed by the applicable Creative Commons License

Table 2. Nitrate detection in commercial bottled water using the proposed bimodal sensor.

Sample	Spiked Nitrate (ppm)	LSV			PEC		
		Found (ppm)	Apparent recovery factor (%)	Relative error %	Found (ppm)	Apparent recovery factor (%)	Relative error %
Levissima 1.3 ppm	0	–	–	–	–	–	–
	10	11.32	101.69	3.02	11.28	98.62	1.58
	20	21.28	98.16	2.80	21.28	98.03	2.80
	30	31.29	99.23	2.87	31.29	99.23	2.87
Uliveto 6.5 ppm	0	6.46	99.37	4.80	6.44	99.09	2.53
	10	16.60	101.54	2.33	16.55	100.77	1.79
	20	26.48	99.70	2.89	26.48	99.64	2.33
	30	36.43	98.94	1.59	36.43	98.94	3.10

Synthesis of Copper Doped g-C_3N_4 Nanosheets

Cu/g-C_3N_4 nanosheets were prepared via in-situ precipitation method. In a 100 mL flask, 0.1 g of the previously synthesized g-C_3N_4 was mixed with the proper amount of $Cu(NO_3)_2.2.5H_2O$ in an aqueous solution and sonicated for half an hour. After the addition of 100 μL of CH_3COOH, the solution was heated to its boiling point. Subsequently, 2 mL of a 1 mol.L^{-1} $NaBH_4$ solution was quickly added to the suspension and reacted for 30 min, accompanied by a large amount of dark precipitate. The resultant precipitates were centrifuged (9,000 rpm, 10 min) and purified with water and ethanol 3 times to get rid of the unbonded Copper. The materials obtained were labelled as X wt.% Cu/g-C_3N_4, with X = 5,10, 20, 30 and 40 where X denotes the nominal metal loading of copper. For comparison, cuprous oxide was prepared by carrying out the same method without adding g-C_3N_4.

Preparation of Cu/g-C_3N_4 Modified FTO Electrode

As shown in Figure 1C, the sensor was prepared on a clean Fluorine-doped Tin Oxide (FTO) glass slide (from Sigma-Aldrich). The conductive glass slides (2×3 cm) were cleaned by sonication in a acetone, ethanol, water and 10% NaOH solution for 10 min each. The supports were then dried with N_2 flux and the nanomaterial, added in 100 mm^3 of PDDA 0.5% solution, was spray-coated on top. The sensor was later dried at 100 °C and stored at room temperature.

Structural and Morphological Characterization

The shown FTIR spectra are the results of 64 accumulation recorded in the range 4000–400 cm^{-1} with a resolution of 4 cm^{-1}. The measurements were conducted on 1 mm^2 samples using a Nicolet 380 spectrometer with a Smart Orbit ATR accessory with a diamond crystal.

TEM images were collected with a JEOL JEM 3010UHR microscope operating at 300 kV. Before the analysis, the material was dispersed in ethanol and deposited on 200 mesh Cu "holey" carbon grids.

Electrochemical Measurements

All the electrochemical measurements were recorded at room temperature with a PGstat30 potentiostat/galvanostat (Autolab, The Netherlands) equipped with FRA module and controlled with NOVA 2.0 software. A standard 3 electrode setup was used, with the modified FTO as WE (immersed area 2 cm^2), saturated KCl Ag/AgCl as RE and Pt wire as CE). Degassing, when working with nitrates, was achieved bubbling N_2 for 15 min.

CV and LSV were conducted in 0.1 M Na_2SO_4 as supporting electrolyte, with a scan rate of 50 and 20 mV s^{-1}, respectively. EIS measurements were conducted at 0.2 V between 0.1 Hz and 100 kHz, with 0.01 V amplitude. 5 mM $[Fe(CN)_6]^{3-/4-}$ was added as redox probe and KCl 0.1 M was selected as supporting electrolyte. The obtained data was processed using Z-View 3.1.

PEC measurements were recorded at 0 V, irradiation was achieved using a Thorlabs LED lamp (M395 L4) powered by a LEDD1B power supply.

Acknowledgements

The authors acknowledge the Italian Ministry of Foreign Affairs and International Cooperation (MAECI) for the grant awarded to Wafa Aidli.

Conflict of Interests

The authors declare no conflict of interest.

Data Availability Statement

The data that support the findings of this study are available from the corresponding author upon reasonable request.

Keywords: Sensor · Nitrates · Photochemistry · Graphitic carbon nitride · Bimodal sensor

[1] M. M. M. Kuypers, H. K. Marchant, B. Kartal, *Nat. Rev. Microbiol.* **2018**, *16*, 263–276.
[2] E. Rembiałkowska, *J. Sci. Food Agric.* **2007**, *87*, 2757–2762.
[3] N. G. Hord, Y. Tang, N. S. Bryan, *Am. J. Clin. Nutr.* **2009**, *90*, 1–10.
[4] R. Poulsen, N. Cedergreen, T. Hayes, M. Hansen, *Environ. Sci. Technol.* **2018**, *52*, 3869–3887.
[5] W. de Vries, *Curr. Opin. Environ. Sci. Heal.* **2021**, *21*, DOI 10.1016/j.coesh.2021.100249.

© 2024 The Authors. ChemElectroChem published by Wiley-VCH GmbH

21960216, 0, Downloaded from https://chemistry-europe.onlinelibrary.wiley.com/doi/10.1002/celc.202300557 by Universita'Degli Studi Di Mila, Wiley Online Library on [27/11/2024]. See the Terms and Conditions (https://onlinelibrary.wiley.com/terms-and-conditions) on Wiley Online Library for rules of use; OA articles are governed by the applicable Creative Commons License

[6] J. Molina, F. J. Jiménez-Jiménez, J. Navarro, E. Ruiz, J. Arenas, F. Cabrera-Valdivia, A. Vázquez, P. Fernández-Calle, L. Ayuso-Peralta, M. Rabasa, F. Bermejo, *J. Neurol. Sci.* **1994**, *127*, 87–89.
[7] M. Ikeda, I. Sato, T. Yuasa, T. Miyatake, S. Murota, *J. Neural Transm.* **1995**, *100*, 263–267.
[8] D. S. Powlson, T. M. Addiscott, N. Benjamin, K. G. Cassman, T. M. de Kok, H. van Grinsven, J.-L. L'hirondel, A. A. Avery, C. van Kessel, *J. Environ. Qual.* **2008**, *37*, 291–295.
[9] M. R. Khan, S. M. Wabaidur, Z. A. Alothman, R. Busquets, M. Naushad, *Talanta* **2016**, *152*, 513–520.
[10] N. Wehbe, M. Jaafar, C. Guillard, J. M. Herrmann, S. Miachon, E. Puzenat, N. Guilhaume, *Appl. Catal. A* **2009**, *368*, 1–8.
[11] H. Gekko, K. Hashimoto, H. Kominami, *Phys. Chem. Chem. Phys.* **2012**, *14*, 7965–7970.
[12] S. Tawkaew, Y. Fujishiro, S. Yin, T. Sato, *Colloids Surf. A* **2001**, *179*, 139–144.
[13] K. T. Ranjit, R. Krishnamoorthy, B. Viswanathan, *J. Photochem. Photobiol. A* **1994**, *81*, 55–58.
[14] Z. Hou, F. Chen, J. Wang, C. P. François-Xavier, T. Wintgens, *Appl. Catal. B* **2018**, *232*, 124–134.
[15] M. Oka, Y. Miseki, K. Saito, A. Kudo, *Appl. Catal. B* **2015**, *179*, 407–411.
[16] H. Wang, M. Li, H. Li, Q. Lu, Y. Zhang, S. Yao, *Mater. Des.* **2019**, *162*, 210–218.
[17] A. Daniel, D. Birot, M. Lehaitre, J. Poncin, *Anal. Chim. Acta* **1995**, *308*, 413–424.
[18] H. Kodamatani, S. Yamazaki, K. Saito, T. Tomiyasu, Y. Komatsu, *J. Chromatogr. A* **2009**, *1216*, 3163–3167.
[19] L. Gao, J. S. Pulido, R. M. Hatfield, R. F. Dundervill, C. A. McCannel, S. A. Shippy, *J. Chromatogr. B* **2007**, *847*, 300–304.
[20] D. A. Cataldo, M. H. Haroon, L. E. Schrader, V. L. Youngs, *Commun. Soil Sci. Plant Anal.* **1975**, *6*, 71–80.
[21] K. K. Karali, L. Sygellou, C. D. Stalikas, *Talanta* **2018**, *189*, 480–488.
[22] M. Farady, *Philos. Trans. R. Soc. London* **1834**, *124*, 77–122.
[23] H. Ryu, D. Thompson, Y. Huang, B. Li, Y. Lei, *Sens. Actuators Rep.* **2020**, *2*, 100022.
[24] S. Cosnier, C. Innocent, Y. Jouanneau, *Anal. Chem.* **1994**, *315*, 147–160.
[25] M. P. N. Bui, J. Brockgreitens, S. Ahmed, A. Abbas, *Biosens. Bioelectron.* **2016**, *85*, 280–286.
[26] M. R. Mahmoudian, Y. Alias, W. J. Basirun, P. Mengwoi, F. Jamali-Sheini, M. Sookhakian, M. Silakhori, *J. Electroanal. Chem.* **2015**, *751*, 30–36.
[27] K. Fajerwerg, V. Ynam, B. Chaudret, V. Garçon, D. Thouron, M. Comtat, *Electrochem. Commun.* **2010**, *12*, 1439–1441.
[28] M. B. Gumpu, N. Nesakumar, B. L. Ramachandra, J. B. B. Rayappan, *J. Anal. Chem.* **2017**, *72*, 316–326.
[29] I. S. Da Silva, W. R. De Araujo, T. R. L. C. Paixão, L. Angnes, *Sens. Actuators B* **2013**, *188*, 94–98.
[30] A. M. Stortini, L. M. Moretto, A. Mardegan, M. Ongaro, P. Ugo, *Sens. Actuators B* **2015**, *207*, 186–192.
[31] B. Hafezi, M. R. Majidi, *Anal. Methods* **2013**, *5*, 3552–3556.
[32] M. Sookhakian, M. A. Mat Teridi, G. B. Tong, P. M. Woi, M. Khalil, Y. Alias, *ACS Appl. Nano Mater.* **2021**, *4*, 12737–12744.
[33] C. Yin, Y. Wang, Q. Zhuang, *J. Electroanal. Chem.* **2021**, *880*, DOI 10.1016/j.jelechem.2020.114817.
[34] N. Xia, D. Wu, T. Sun, Y. Wang, X. Ren, F. Zhao, L. Liu, X. Yi, *Sens. Actuators B* **2021**, *327*, 128913.
[35] Q. Han, C. Wang, P. Liu, G. Zhang, L. Song, Y. Fu, *Sens. Actuators B* **2021**, *330*, 129388.
[36] H. Deng, Y. Chai, R. Yuan, Y. Yuan, *Anal. Chem* **2020**, *92*, 8370.
[37] W. Aidli, V. Pifferi, A. Mars, D. Marinotto, M. Longhi, A. Manfredi, A. H. Hamzaoui, L. Falciola, *Electrochim. Acta* **2023**, *464*, 142936.
[38] J. Jia, W. Lu, L. Li, Y. Gao, Y. Jiao, H. Han, C. Dong, S. Shuang, *J. Mater. Chem. B* **2020**, *8*, 2123–2127.
[39] H. Shang, H. Xu, L. Jin, C. Chen, T. Song, C. Wang, Y. Du, *Sens. Actuators B* **2019**, *301*, 127060.
[40] H. Han, G. Ding, T. Wu, D. Yang, T. Jiang, B. Han, *Molecules* **2015**, *20*, 12686–12697.
[41] D. Nandi, S. Siwal, K. Mallick, *New J. Chem.* **2017**, *41*, 3082–3088.
[42] C. Cometto, A. Ugolotti, E. Grazietti, A. Moretto, G. Bottaro, L. Armelao, C. Di Valentin, L. Calvillo, G. Granozzi, *NPJ 2D Mater. Appl.* **2021**, *5*, 63.
[43] P. Huang, J. Huang, S. A. Pantovich, A. D. Carl, T. G. Fenton, C. A. Caputo, R. L. Grimm, A. I. Frenkel, G. Li, *J. Am. Chem. Soc.* **2018**, *140*, 16042–16047.
[44] V. Sudha, G. Murugadoss, R. Thangamuthu, *Sci. Rep.* **2021**, *11*, 1–12.
[45] X. Xi, X. Peng, C. Xiong, D. Shi, J. Zhu, W. Wen, X. Zhang, S. Wang, *Microchim. Acta* **2020**, *187*, DOI 10.1007/s00604-020-04373-w.
[46] J. Mu, J. Li, X. Zhao, E. C. Yang, X. J. Zhao, *RSC Adv.* **2016**, *6*, 35568–35576.
[47] Y. Zhou, L. Zhang, W. Wang, *Nat. Commun.* **2019**, *10*, 1–8.
[48] J. Liang, Y. Zheng, Z. Liu, *Sens. Actuators B* **2016**, *232*, 336–344.
[49] A. K. M. S. Inam, M. A. Costa Angeli, B. Shkodra, A. Douaki, E. Avancini, L. Magagnin, L. Petti, P. Lugli, *ACS Omega* **2021**, *6*, 33523–33532.
[50] B. Patella, R. R. Russo, A. O'Riordan, G. Aiello, C. Sunseri, R. Inguanta, *Talanta* **2021**, *221*, 121643.
[51] A. Gutés, C. Carraro, R. Maboudian, *Electrochim. Acta* **2013**, *103*, 38–43.
[52] C. Hyusein, V. Tsakova, *J. Electroanal. Chem.* **2023**, *930*, DOI 10.1016/j.jelechem.2023.117172.
[53] F. Can, S. Korkut Ozoner, P. Ergenekon, E. Erhan, *Mater. Sci. Eng. C* **2012**, *32*, 18–23.
[54] S. M. Sibug-Torres, L. P. Go, V. C. G. Castillo, J. L. R. Pauco, E. P. Enriquez, *Anal. Chim. Acta* **2021**, *1160*, 338430.
[55] X. Li, X. Zhang, H. Ma, D. Wu, Y. Zhang, B. Du, Q. Wei, *Biosens. Bioelectron.* **2014**, *55*, 330–336.

Manuscript received: October 16, 2023
Revised manuscript received: December 21, 2023
Version of record online: ■■, ■■

© 2024 The Authors. ChemElectroChem published by Wiley-VCH GmbH

21960216, 0, Downloaded from https://chemistry-europe.onlinelibrary.wiley.com/doi/10.1002/celc.202300557 by Universita'Degli Studi Di Mila, Wiley Online Library on [27/11/2024]. See the Terms and Conditions (https://onlinelibrary.wiley.com/terms-and-conditions) on Wiley Online Library for rules of use; OA articles are governed by the applicable Creative Commons License

RESEARCH ARTICLE

An innovative bimodal sensor, based on copper-modified graphitic carbon nitride (g-C_3N_4) was proposed for the analytical determination of nitrates. After the characterization of the material, coherent electrochemical and photoelectrochemical measurements were performed in the presence of interferents and in real water samples.

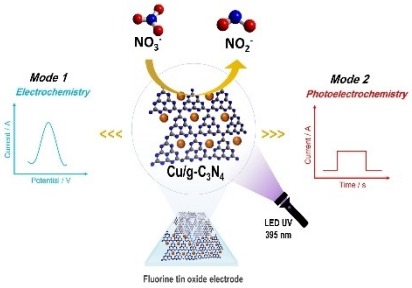

W. Aidli, D. Fumagalli, H. Helli, L. Falciola*, V. Pifferi*

1 – 10

Electrochemical and Photoelectrochemical Bimodal Sensor Based on Copper Modified g-C_3N_4 for Nitrate Detection

21960216, 0, Downloaded from https://chemistry-europe.onlinelibrary.wiley.com/doi/10.1002/celc.202300557 by Universita'Degli Studi Di Mila, Wiley Online Library on [27/11/2024]. See the Terms and Conditions (https://onlinelibrary.wiley.com/terms-and-conditions) on Wiley Online Library for rules of use; OA articles are governed by the applicable Creative Commons License

ChemElectroChem

Supporting Information

Electrochemical and Photoelectrochemical Bimodal Sensor Based on Copper Modified g-C_3N_4 for Nitrate Detection

Wafa Aidli,* Daniele Fumagalli, Hanieh Helli, Luigi Falciola,* and Valentina Pifferi

Electrochemical and Photoelectrochemical bimodal sensor based on Copper modified g-C_3N_4 for Nitrate detection

Wafa Aidli*, Daniele Fumagalli, Hanieh Helli, Elisabetta Inico, Luigi Falciola*, Valentina Pifferi

Wafa Aidli, Daniele Fumagalli, Hanieh Helli, Elisabetta Inico, Luigi Falciola, Valentina Pifferi
Electroanalytical Chemistry Group, Department of Chemistry
Università degli Studi di Milano
Via Golgi 19, 20133, Milano, Italy
E-mail: wafa.aidli@unimi.it; luigi.falciola@unimi.it
Homepage url: sites.unimi.it/ELAN

SUPPORTING INFORMATION

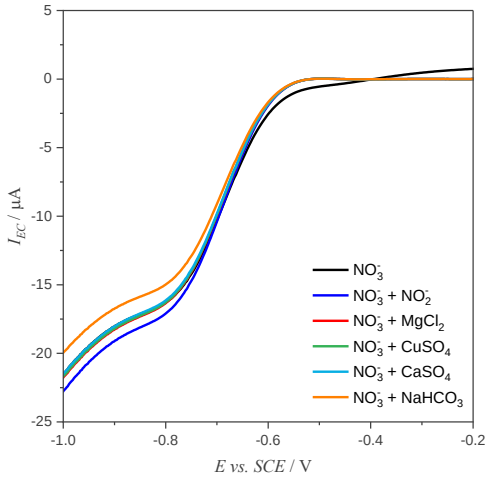

Figure S1 – LSV measurements in the presence of interferents

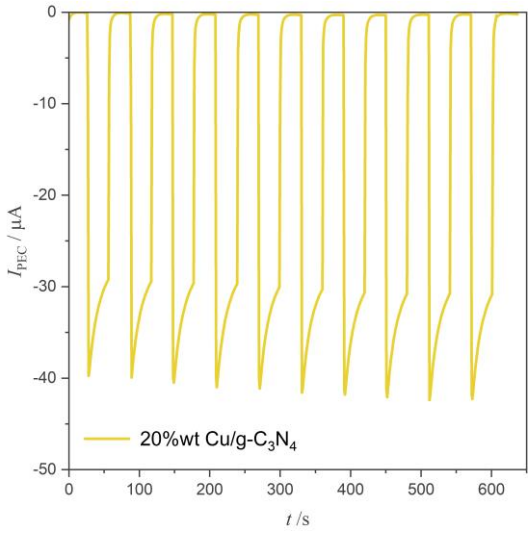

Figure S2 – Stability of the photocurrent response obtained with multiple light on - light off cycles.

Table S1 EIS mathematical parameters.

Electrode	R_{Ω} (Ω cm^2)	CPE_{dl} ($\mu F.cm^{-2}$)	α_{dl} (s)	R_{ct} ($K\Omega$ cm^2)	Z_w ($K\Omega$ cm^2)	τ_w	α_w
bare FTO	79.02	3.05	0.98	4,81	11.06	36.96	0.5
g-C_3N_4	59.78	3.85	0.97	6.52	0.01	0.0015	0.34
Cu_2O	52.42	5.06	0.96	0.72	9.978	51.61	0.5
5wt%Cu/g-C_3N_4	54.12	4.12	0.97	1.59	11.8	110.3	0.5
10wt%Cu/g-C_3N_4	34.30	6.71	0.93	1.34	39.11	95.49	0.5
20wt%Cu/g-C_3N_4	41.46	14.88	0.86	0.43	12.96	49.18	0.5
30wt%Cu/g-C_3N_4	46.10	15.08	0.87	0.40	5.01	6.512	0.5
40wt%Cu/g-C_3N_4	46.30	7.90	0.90	1.09	20.15	82.62	0.5